NUCLEAR SCIENCE AND ENGINEERING: **177**, 350–360 (2014)

High-Dimensional Model Representations for the Neutron Transport Equation

Zhengzheng Hu, Ralph C. Smith,* Jeffrey Willert, and C. T. Kelley

North Carolina State University, Department of Mathematics
Raleigh, North Carolina 27695

Received June 26, 2013
Accepted October 29, 2013
http://dx.doi.org/10.13182/NSE13-52

Abstract—*The Boltzmann transport equation is used to model the neutron flux in a nuclear reactor. The solution of the transport equation is the neutron flux, which depends on a large number of material cross sections that can be on the order of thousands. These cross sections describe various types of possible interactions between neutrons, such as fission, capture, and scattering. The cross sections are measured experimentally and therefore have associated uncertainties. It is thus necessary to quantify how the uncertainty of the cross-section values is propagated through the model for the neutron flux. High-dimensional model representations (HDMRs) can be employed to systematically quantify input-output relations. It can, however, be computationally prohibitive to construct a surrogate model using the HDMR framework for a model that has thousands of parameters. In this paper, we introduce an algorithm that utilizes the New Morris Method to first reduce the parameter space to include only the significant individual and pairwise effects and then construct a surrogate model using a Cut-HDMR expansion within the reduced space. A unified index is introduced to facilitate the comparison of the significance of the model parameters. The accuracy and efficiency of the surrogate model is demonstrated using a one-dimensional neutron transport equation.*

I. INTRODUCTION

Simulation-based models are presently being developed to serve as "virtual reactors" that can be used to predict the behavior of the nuclear materials, neutron transport, heat transfer, and thermal-hydraulic components of a reactor using limited experimental measurements. These simulations can then be used to improve the nuclear reactor efficiency, reduce operating costs, and enhance reactor safety. Such models depend on a large number of input parameters. For example, the Boltzmann transport equation, which is used to quantify the neutron distributions in a nuclear reactor, often depends on thousands of cross-section values. In many cases, the values of the input parameters cannot be accurately measured through experiments, or only the ranges of the parameters can be provided through experiments. This means that the parameter values have associated uncertainties that must be quantified and propagated through models.

Monte Carlo (MC) simulations are commonly used to assess the uncertainty of the parameters. It is straightforward to perform MC simulations, but they will be prohibitively expensive if the underlying model depends on a large number of inputs or if the underlying model is computationally expensive, which is the case for nuclear models. High-dimensional model representations (HDMRs) have been introduced to systematically identify the relationships between sets of inputs (e.g., parameters) and outputs (responses); see the general review by Rabitz and Alis[1] and the references cited therein. HDMRs express the model output as a finite additive sum of correlated functions with increasing numbers of input variables up to the total number of inputs. The resultant HDMR expansions can be used as a reduced-order surrogate model that depends on fewer parameters and, more importantly, fewer coupled parameters (interactions among parameters) and is therefore more efficient than the original full model.

*E-mail: rsmith@ncsu.edu

Depending on the research focus, components of the reactor core are initially modeled separately. In this work, we consider the neutron transport equation that focuses on quantifying the neutron distributions in the reactor core. We propose and demonstrate an algorithm that can be used to efficiently and accurately identify the relationships between input parameters (cross sections) and the response [effective eigenvalue of the one-dimensional (1-D) neutron transport equation]. A surrogate model will be built using the HDMR expansions whose accuracy will also be discussed.

We focus on a steady-state, 1-D, monoenergetic neutron transport model posed on a homogeneous, planar geometry. This model illustrates many of the issues that must be addressed when determining influential parameters and constructing surrogate models for reactor simulations while providing the numerical efficiency required to evaluate the accuracy of the proposed method. The limitations of using this simplified model and future extensions to three-dimensional (3-D) models and codes are detailed in Sec. VII.

HDMR was originally proposed as a framework to construct a fully equivalent operational model of complex chemical systems; see Refs. 1 through 4 for examples. Since its development, it has been used to construct computational models directly from laboratory data, perform quantitative risk assessment, identify key model parameters, analyze global uncertainty, etc. There are two commonly used expansions: ANOVA-HDMR and Cut-HDMR, which depend on how the hierarchical functions are evaluated. ANOVA-HDMR, which is often used to analyze global sensitivity, is basically the same as the analysis of variance decomposition (ANOVA). It involves high-dimensional integration that is computationally expensive to evaluate. Cut-HDMR, on the other hand, is evaluated along the so-called cut lines or hyperplanes with respect to preselected reference points in the domain of the inputs, and thus, it is more computationally efficient than ANOVA-HDMR. Moreover, it is often argued that the high-order interactions among inputs are weak in many physical problems and therefore can be omitted from the HDMR expansion. However, the accuracy of the truncated Cut expansion heavily depends on the choice of the reference point. It is often optimal to choose the reference point to be the mean value of the inputs[5–7] if only up to the second-order interactions are included.

For a problem with a large number of parameters, it can still be computationally expensive to construct a second-order Cut-HDMR expansion. To make it more computationally feasible, we proposed an algorithm that screens the input space for significant inputs and interactions and then adopts the Cut-HDMR expansion in the reduced parameter space. The screening algorithm follows from the New Morris Method[8,9] and is capable of identifying both individual inputs and pairwise interactions. A unified index is defined for both first- and second-order effects to facilitate the comparison of the parameters. A different sampling strategy is employed to calculate the second-order effects. The applicability of the algorithm is demonstrated for the 1-D neutron transport equation.

We note that the second-order HDMR expansions employed here are not the only second-order method that has been used for surrogate model construction and uncertainty propagation for input-output relations of the form

$$y = f(q) ,$$

where $q = (q_1, \cdots, q_p)$ denotes the p inputs or parameters and y are responses or quantities of interest.

The goal with all such expansions is to construct representations

$$f(q) = f_0 + \sum_{i=1}^{p} f_i(q_i) + \sum_{1 \le i_1 < i_2 \le p} f_{i_1, i_2}(q_{i_1}, q_{i_2})$$

for nonlinear problems where high-order interactions are weak or negligible. As detailed in Rabitz and Alis,[1] the evaluation of the hierarchical functions f_0,f_i, and f_{i_1, i_2} requires numerical integration over the entire parameter space if one employs ANOVA-HDMR whereas it is shown in Sec. III that these computations can be reduced to function evaluations at anchor or reference points $\bar{q}$ if one employs Cut-HDMR. This vast improvement in efficiency comes at the cost of reduced accuracy and lack of global convergence criteria. Alternatively, for the perturbation methods detailed in Refs. 10 and 11, one constructs f_0,f_i, and f_{i_1, i_2}, which are no longer hierarchical, using a second-order Taylor expansion of $f(q)$ at a nominal parameter value $\bar{q}$. The perturbation method requires that derivatives of f be approximated, which can render the method both more accurate and more computationally intensive than Cut-HDRM. The accuracy of Cut-HDMR is often improved through the use of multiple anchor points. A numerical comparison between Cut-HDMR and the second-order perturbation expansions goes beyond the scope of this paper and constitutes future research. We note that the proposed algorithm differs significantly from the perturbation methods of Refs. 10 and 11 in the use of the New Morris Method to ascertain a subset of influential parameters prior to surrogate model construction.

The rest of the paper is organized as follows. We briefly summarize the 1-D neutron transport equation and the numerical method in Sec. II. In Sec. III, the Cut-HDMR expansion is discussed. The screening algorithm used to identify both the significant inputs and interactions is presented in Sec. IV. We summarize the Cut-HDMR expansion in the reduced input space in Sec. V. In Sec. VI, we demonstrate the capability of the proposed algorithm using the 1-D neutron transport problem. Concluding remarks are summarized in Sec. VII.

II. k-EIGENVALUE PROBLEM OF THE 1-D NEUTRON TRANSPORT EQUATION

We consider a 1-D k-eigenvalue problem for steady-state, monoenergetic, isotropically scattering neutron transport in homogeneous planar (commonly referred as slab) geometry. The governing equation is

$$\mu\frac{\partial\psi}{\partial x}(x,\mu)+\Sigma_t\psi(x,\mu)-\frac{\Sigma_s}{2}\phi(x)=\frac{\nu}{2k}\Sigma_f\phi(x)\ , \qquad (1)$$

where

$\psi(x,\mu)$ = azimuthally integrated angular flux

$\phi(x)$ = scalar flux; i.e., $\phi(x)=\int_{-1}^{1}\psi(x,\mu)d\mu$

$\Sigma_t, \Sigma_s, \Sigma_f$ = macroscopic total, scattering, and fission cross sections (m^{-1}), respectively,

and where $x\in[0,L]$ and the polar cosine $\mu\in[-1,1]$. We note that the total cross section is defined by $\Sigma_t=\Sigma_s+\Sigma_f+\Sigma_c$, where Σ_c is the macroscopic capture cross section (m^{-1}).

We assume no incoming flux on the left or right boundaries, i.e., vacuum boundary conditions. The boundary conditions prescribe the incident angular fluxes on the left and right edges of the slab and are taken to be

$$\psi(0,\mu)=0 \quad \text{for } \mu>0$$

and

$$\psi(L,\mu)=0 \quad \text{for } \mu<0\ .$$

Equation (1) is solved numerically using a MATLAB code developed by Willert and Kelley (http://www4.ncsu.edu/~ctk/). More specifically, the governing equation is represented at a finite set of polar cosine values μ_j with associated weights w_j for $j=1,\cdots,N_\mu$:

$$\mu_j\frac{\partial\psi_j}{\partial x}(x)+\Sigma_t\psi_j(x)-\frac{\Sigma_s}{2}\phi(x)=\frac{\nu}{2k}\Sigma_f\phi(x)\ ,$$

and the scalar flux is approximated by

$$\phi(x)=\sum_{j=1}^{N_\mu}w_j\psi_j(x)\ .$$

If we define the loss L and production P operators as

$$\begin{aligned}L\psi &\equiv \mu\frac{\partial\psi}{\partial x}(x)+\Sigma_t\psi(x)-\frac{\Sigma_s}{2}\phi(x)\\ &= \mu\frac{\partial\psi}{\partial x}(x)+\Sigma_t\psi(x)-\frac{\Sigma_s}{2}\int_{-1}^{1}\psi(x,\mu)d\mu\end{aligned}$$

and

$$P\psi\equiv\frac{\nu}{2}\Sigma_f\phi(x)=\frac{\nu}{2}\Sigma_f\int_{-1}^{1}\psi(x,\mu)d\mu\ ,$$

the k-eigenvalue problem can then be written as

$$L\psi=\frac{1}{k}P\psi\ .$$

In space, the diamond-difference discretization is used, so the angular flux is evaluated at cell faces. More specifically, the discretized loss L_i and production P_i operators are

$$\begin{aligned}L_i\psi_j \equiv\ & \mu_j\frac{\psi_{j,i+1/2}-\psi_{j,i-1/2}}{\Delta x}+\Sigma_t\frac{\psi_{i,i+1/2}+\psi_{j,i-1/2}}{2}\\ &-\frac{\Sigma_s}{2}\sum_{\ell=1}^{N_\mu}w_\ell\psi_{\ell,i}\end{aligned}$$

and

$$P_i\psi_j\equiv\frac{\nu}{2}\Sigma_f\sum_{\ell=1}^{N_\mu}w_\ell\psi_{\ell,i}\ .$$

The discretized system is then solved using power iteration[12,13] (PI), and the scheme at the $(n+1)$'th iteration is

$$L_i\psi_j^{n+1}=\frac{1}{k_{eff}^n}P_i\psi_j^n$$

and

$$k_{eff}^{n+1}=k_{eff}^n\frac{\int\nu\Sigma_f\phi^{n+1}dx}{\int\nu\Sigma_f\phi^n dx}$$

for $j=1,\cdots,N_\mu$ and $i=1,\cdots,N_x$, where N_x is the number of grid points along x. Here, k_{eff} is the largest eigenvalue of the operator $L^{-1}P$ and is called the multiplication factor. This eigenvalue indicates the time dependence of the neutron density in the nuclear reactor. The reactor is termed subcritical (neutron density decreases in time) if $k_{eff}<1$, critical (density remains constant) if $k_{eff}=1$, and supercritical (density increases in time) if $k_{eff}>1$. Therefore, the eigenvalue is of great practical importance and is the desired output of most reactor eigenvalue calculations.

To simplify the notation, let us denote that $k_{eff}=f(q)$, where the function f is the 1-D transport equation whose solution is k_{eff}. The input vector q is the collection of all three cross sections; i.e., $q=(\Sigma_s^{N_x},\Sigma_c^{N_x},\Sigma_f^{N_x})$. Here, $\Sigma_s^{N_x},\Sigma_c^{N_x},\Sigma_f^{N_x}$ are the discretized scattering, capture, and fission cross sections, respectively, and each of them has N_x elements (on the order of hundreds to thousands). Therefore, the total number of inputs is $3N_x>500$.

III. CUT-HDMR

The essence of the HDMR expansions is to express the response in terms of hierarchical correlated function expansions.[1,4,5,14] Depending on the exact form of the hierarchical functions, there are two types of expansions: ANOVA and Cut. Since the ANOVA expansion involves

high-dimensional integration that can be computationally prohibitive, we consider the Cut expansion in which case the hierarchical functions are evaluated along the so-called cut lines or planes or hyperplanes with respect to the preselected reference point in the domain of the inputs.

We consider a multivariate function

$$f(q)=f(q_1,q_2,\cdots,q_p)$$

defined on the p-dimensional domain Ω_p and a prechosen anchor point $\bar{q}=(\bar{q}_1,\bar{q}_2,\cdots,\bar{q}_p)\in\Omega_p$. The Cut-HDMR then takes the form[1]

$$\begin{aligned} f(q)=f_0+\sum_{i=1}^{p} f_i(q_i) &+\sum_{1\le i_1<i_2\le p} f_{i_1 i_2}(q_{i_1},q_{i_2})+\cdots \\ &+\sum_{1\le i_1<\cdots<i_s\le p} f_{i_1\cdots i_s}(q_{i_1},\cdots,q_{i_s})+\cdots \\ &+f_{12\cdots p}(q_1,\cdots,q_p)\ , \end{aligned}$$

where

$$\begin{aligned} f_0 &= f(\bar{q})\ , \\ f_i(q_i) &= f(q)|_{q=\bar{q}\setminus q_i}-f_0\ , \end{aligned}$$

and

$$f_{ij}(q_i,q_j)=f(q)|_{q=\bar{q}\setminus\{q_i,q_j\}}-f_i(q_i)-f_j(q_j)-f_0-\cdots\ .$$

The notation $q=\bar{q}\setminus q_U$ means that the components of q other than those indices that belong to the set U are set equal to those of the anchor point. For example,

$$q=\bar{q}\setminus\{q_i,q_j\}=(\bar{q}_1,\cdots,\bar{q}_{i-1},q_i,\cdots,\bar{q}_{j-1},q_j,\bar{q}_{j+1},\cdots,\bar{q}_p)\ .$$

The truncated Cut-HDMR expansion

$$f(q)=f_0+\sum_{i=1}^{p} f_i(q_i)+\sum_{1\le i_1<i_2\le p} f_{i_1 i_2}(q_{i_1},q_{i_2})$$

is often used without significantly degrading accuracy since the high-order interactions among inputs are weak for most physical systems.[5–7]

We note that the zeroth-order f_0 is evaluated at the reference point, which requires one model evaluation. The first-order term $f_i(q_i)$ is evaluated along a cut line, and the second-order terms $f_{ij}(q_i,q_j)$ are evaluated on a cut plane. Therefore, they can be approximated by 1-D and 2-D Lagrange interpolating polynomials. More specifically, the first-order terms for an arbitrary point q_i^{new} can be evaluated using

$$f(q_i^{new})=\sum_{k=1}^{N_L}\phi_k(q_i^{new})f(\bar{q}_1,\cdots,\bar{q}_{i-1},q_i^k\cdots,\bar{q}_p)-f_0\ ,$$

where $\{q_i^k\}_{k=1}^{N_L}$ for $i=1,\cdots,p$ are the interpolation points and the Lagrange interpolating polynominal $\phi_k(q_i)$ is defined as

$$\phi_k(q_i)=\prod_{\substack{0\le m\le N_L\\ m\ne k}}\frac{q_i-q_i^m}{q_i^k-q_i^m}\ .$$

Similarly, the second-order terms for arbitrary points q_i^{new} and q_j^{new} can be evaluated using

$$\begin{aligned} f_{ij}(q_i^{new},q_j^{new}) &= \sum_{k_1=1}^{N_L}\sum_{k_2=1}^{N_L}\phi_{k_1k_2}(q_i^{new},q_j^{new}) \\ &\quad\times f(\bar{q}_1,\cdots,\bar{q}_{i-1},q_i^{k_1}\cdots,\bar{q}_{j-1},q_j^{k_2}, \\ &\quad\bar{q}_{j+1},\cdots,\bar{q}_p), \\ &\quad -f_i(q_i^{new})-f_j(q_j^{new})-f_0 \end{aligned}$$

where $\phi_{k_1k_2}(q_i,q_j)=\phi_{k_1}(q_i)\otimes\phi_{k_2}(q_j)$. Therefore, the number of function calls required to calculate all the first-order terms is $p(N_L-1)$, and the number of function calls required to evaluate all second-order terms is $p(p-1)(N_L-1)^2/2$. We note that if three interpolation points are used ($N_L=3$) for a system with 500 parameters ($p=500$), the number of function evaluations to calculate all the second-order terms is 499 000, which is significant. To reduce the computational cost, we employ the New Morris Method[8,9] to reduce the parameter space so that it includes only the significant individual and pairwise effects.

IV. NEW MORRIS METHOD

Morris screening was originally proposed by Morris[15] to efficiently explore the global sensitivity of inputs. Campolongo and Saltelli[16] later suggested a modification aimed at improved exploration of the input space. Basically, for any input q selected in the parameter space, the local sensitivity of each parameter, or the elementary effect, is approximated by its finite difference approximation

$$\frac{\partial f(q)}{\partial q_i}=\frac{f(q_1,\cdots,q_i+h_i,\cdots,q_p)-f(q)}{h_i}\ , \qquad (2)$$

where h_i is a preselected step size such that $(q_1,\cdots,q_i+h_i,\cdots,q_p)$ is still inside the parameter space. Multiple input vectors can be then selected to construct a distribution whose sample mean and standard deviation can be used to analyze the global sensitivity of each parameter. A parameter with either a large mean or standard deviation will be considered to be significant.

The unique thing about the Morris screening procedure is that through the construction of a sampling matrix, an "optional" trajectory for calculating the local sensitivity of all inputs is established. Therefore, it is the most efficient way to explore the input space. Figure 1 demonstrates a possible trajectory based on the sampling matrix for two inputs.

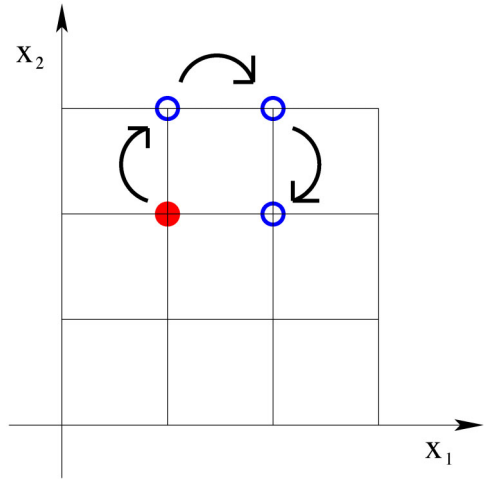

Fig. 1. Sketch of the trajectory in two dimensions proposed by Campolongo and Saltelli.[16] Solid red dot: reference point; blue circles: points on the trajectory used to calculate the elementary effects.

Morris[15] and Campolongo and Saltelli[16] considered only the first-order screening that screens for the significant individual effects only. Campolongo and Braddock[8] later introduced the New Morris Method as an extension to the Morris screening so that the pairwise effects can also be evaluated. The capability of the method was demonstrated by Cropp and Braddock.[9]

The goal of the second-order screening is to evaluate all pairwise effects between parameters. For any input q selected in the parameter space, the local pairwise effect, or the second-order elementary effect, can be approximated by

$$\frac{\partial^2 f(q)}{\partial q_i \partial q_j} = \frac{f(q_1,\cdots,q_i+h_i,\cdots,q_j+h_j,\cdots,q_p)}{h_i h_j} - \frac{f(q_1,\cdots,q_i+h_i,\cdots,q_p)}{h_i h_j} - \frac{f(q_1,\cdots,q_j+h_j,\cdots,q_p)-f(q)}{h_i h_j},$$

where h_i, h_j are preselected step sizes such that $(q_1,\cdots,q_i+h_i,\cdots,q_j+h_j,\cdots,q_p)$ is still inside the parameter space. Similar to the first-order screening, multiple input vectors can be then selected to construct a distribution whose sample mean and standard deviation can be used to analyze the global sensitivity due to the interactions among parameters. A pair with either a large mean or standard deviation will be considered to be significant.

To evaluate all second-order effects efficiently, the New Morris Method[8] uses a graph theory-based strategy to construct the sampling matrices and is an order p^2 method (i.e., the number of model evaluations required to calculate the second-order effects is on the order of p^2). We introduce a different sampling strategy that is also an order p^2 method but is more efficient for $p>5$. We will first summarize the Morris screening (the first-order screening) in Sec. IV.A and then discuss the second-order screening in more detail in Sec. IV.B.

IV.A. Morris Screening

Consider a response function $f(q)$ that depends on p input factors: $f(q)=f(q_1,q_2,\cdots,q_p)$, with $q_i \in [\ell b_i, ub_i]$ for $i=1,2,\cdots,p$. We demonstrate here how to construct the level ℓ Morris screening sampling matrices of first and second order. Here, ℓ is a positive integer ($\ell>1$) that defines the number of partitions in the input space. To simplify the notation, the sampling matrices will be defined on the scaled input factors $x=(x_1,x_2,\cdots,x_p)$, where x_i assumes integer values on the interval $[0,\ell-1]$ for $i=1,2,\cdots,\ell$. A simple linear function will map x to the original input q: $q_i=\ell b_i+x_i(ub_i-\ell b_i)/(\ell-1)$.

IV.A.1. Construction of the First-Order Sampling Matrix

The first-order Morris sampling matrix for a p-dimensional factor vector x is a $(p+1)\times p$ matrix that has the property that there are two rows of the matrix that differ only in their i'th entries for $i=1,2,\cdots,p$. Here are steps to construct such a matrix, A^*.

Algorithm M1:

1. Construct matrix A: strictly lower triangular of 1's with size $(p+1)\times p$:

$$A=\begin{pmatrix} 0 & 0 & 0 & \cdots & 0 \\ 1 & 0 & 0 & \cdots & 0 \\ 1 & 1 & 0 & \cdots & 0 \\ \vdots & \vdots & \vdots & \ddots & \vdots \\ 1 & 1 & 1 & \cdots & 1 \end{pmatrix}.$$

2. Select the increment Δ, which is the step size. Δ is a positive integer, and $\Delta<\ell-1$.

3. Randomly select a starting vector x^* with p elements from the set $\{0,1,2,\ell-1-\Delta\}$.

4. Define a matrix D^*, p-dimensional diagonal matrix of integers, whose diagonal elements are selected from the set $\{-1,1\}$ with equal probability.

5. Calculate A^*: $A^*=(J_{p+1,1}x^*+\Delta/2[(2A-J_{p+1,p})D^*+J_{p+1,p}])P^*$, where $J_{m,n}$ is an $m\times n$ matrix of 1's, P^* is a $p\times p$ random permutation matrix, i.e., a matrix obtained by randomly permuting columns of a $p\times p$ identity matrix.

IV.A.2. First-Order Elementary Effect

Having constructed the first-order sampling matrix A^*, it is straightforward to calculate the first-order elementary effect (2). We denote the first-order sampling matrix for the original input factors as C^*. Here, the columns of the matrix C^*, C_i^*, can be readily calculated using the relation

$$C_i^* = \ell b_i + A_i^*(ub_i - \ell b_i)/(\ell - 1) \quad \text{for } i = 1, 2, \cdots, p ,$$

where $\{A_i^*\}_{i=1}^k$ are columns of the first-order sampling matrix defined in *Algorithm M1*.

Let the i'th row of C^* be $C^*(i) = [c_{i1}, c_{i2}, \cdots, c_{is}, \cdots, c_{ip}]$, which is different from the j'th row of C^* only at s'th entry; i.e., $C^*(j) = [c_{i1}, c_{i2}, \cdots, c_{js}, \cdots, c_{ip}]$. The first-order elementary effect for the s'th component can then by calculated by

$$d_{ss} = \frac{f(C^*(i)) - f(C^*(j))}{c_{is} - c_{js}} . \tag{3}$$

We note that the number of function evaluations needed to calculate all p first-order significance indices is $(p+1)$ times.

IV.B. Second-Order Screening

IV.B.1. Construction of the Second-Order Sampling Matrix

We propose *Algorithm M2* to construct a sampling matrix for the second-order screening. Using the constructed matrix, all pairwise interactions will be explored using the same strategy that Morris screening uses.

The goal is to construct a $p \times p$ matrix B^* that has a property that there are two rows of the matrix that differ only in their i'th and j'th entries for $i, j = 1, 2, \cdots, p$.

Algorithm M2:

1. Construct a $p \times p$ matrix B that is composed of a $(p-1) \times (p-1)$ identity matrix and whose first row is a zero vector and elements 2 through p in the first column are all 1's:

$$B = \begin{pmatrix} 0 & 0 & 0 & \cdots & 0 \\ 1 & 1 & 0 & \cdots & 0 \\ 1 & 0 & 1 & \cdots & 0 \\ \vdots & \vdots & \vdots & \ddots & \vdots \\ 1 & 0 & 0 & \cdots & 1 \end{pmatrix} .$$

2. Select the increment Δ, which is the step size. Δ is a positive integer, and $\Delta < \ell - 1$.

3. Randomly pick a starting vector x^* with k elements from the set $\{0, 1, 2, \ell - 1 - \Delta\}$.

4. Define a matrix D^*, p-dimensional diagonal matrix of integers, whose elements are selected from the set $\{-1, 1\}$ with equal probability.

5. The second-order sampling matrix B^* is defined by

$$B^* = (J_{p,1} x^* + \Delta/2[(2B - J_{p,p})D^* + J_{p,p}])P^* ,$$

where $J_{m,n}$ and P^* are defined in step 5 of *Algorithm M1*.

Note that steps 2, 3, and 4 are identical to those of *Algorithm M1*. One of the properties of the matrix B is that there is only one element that is different from the rest of the elements for each column. Since B^* is a randomized version of B, it has the same property. This property can be used to expedite the evaluations of the second-order elementary effects, which is explained in the next section.

IV.B.2. Second-Order Elementary Effect

We denote the second-order sampling matrix for the original input factors by G^* (transformed from B^* constructed using *Algorithm M2* to reflect the scales of the original parameters). We denote the m'th row of G^* by

$$G^*(m) = [g_{m1}, \cdots, g_{ms}, \cdots, g_{mv}, \cdots, g_{mp}] ,$$

which is different from the n'th row of G^* only at v'th and s'th entries; i.e.,

$$G^*(n) = [g_{m1}, \cdots, g_{ns}, \cdots, g_{nv}, \cdots, g_{mp}] .$$

The second-order elementary effect between the s'th and v'th components can then by calculated by

$$d_{sv} = \frac{f(G^*(m)) - f(g_{m1}, \cdots, g_{ms}, \cdots, g_{nv}, \cdots, g_{mp})}{(g_{ms} - g_{ns})(g_{mv} - g_{nv})} - \frac{f(g_{m1}, \cdots, g_{ns}, \cdots, g_{mv}, \cdots, g_{mp}) - f(G^*(n))}{(g_{ms} - g_{ns})(g_{mv} - g_{nv})} . \tag{4}$$

Here, the sampling matrix G^* can be used to evaluate the first and last terms in Eq. (4). Because of the construction of the second-order sampling matrix, one of the two middle terms in Eq. (4) is shared by all second-order effects. Using the matrix B in *Algorithm M2* as an example, it is straightforward to see that the input vector that is shared by all pairwise effect calculations is $(1, 0, 0, \cdots, 0)$. Therefore, only one of the two middle terms in Eq. (4) needs to be calculated for each pair. Since the number of pairwise interactions is $p(p-1)/2$, the number of functions evaluations required is $p + p(p-1)/2 + 1 = p(p+1)/2 + 1$ to construct all second-order elementary effects. Therefore, this sampling

strategy is an order p^2 method. It is more efficient than that used in the New Morris Method[8] if $p>5$. Moreover, *Algorithm M2* is almost identical to that of the Morris screening and is efficient to implement. The only difference is that it starts with a different matrix.

Suppose that the screening is performed r times and the corresponding elementary effects are d^i for $i=1,\cdots,r$, and $d^i=\{d^i_{sv}\}^p_{s,v=1}$. We can then calculate the sample mean M and sample standard deviation S of the elementary effects:

$$M=\{M_{sv}\}^p_{s,v=1}=\frac{1}{r}\sum_{i=1}^{r}d^i$$

and

$$S=\{S_{sv}\}^p_{s,v=1}=\left(\sum_{i=1}^{r}(d^i-M).\times(d^i-M)/(r-1)\right)^{1/2}. \tag{5}$$

Note that d^i and M are matrices, so $.\times$ is used to indicate the component-wise multiplication. The diagonal elements of M and S reflect the means and standard deviations of the first-order effects, respectively. The off-diagonal elements reflect those of the second-order effects.

Motivated by Campolongo and Saltelli,[16] we measure the statistical significance of the inputs and interactions by the distance from the origin to the (M,S) plane. Let us denote the statistical significance index by *SIG*:

$$SIG=\{SIG_{sv}\}^p_{s,v=1}=\sqrt{M.\times M+S.\times S}\ .$$

Since our goal is to select the most significant individual and pairwise effects and incorporate them into the Cut-HDMR expansion, we normalize the *SIG* in terms of the maximum of the diagonal and off-diagonal elements to facilitate the comparison:

$$SIG^*=\begin{cases}\dfrac{SIG_{ss}}{\max_s SIG_{ss}}, & s=1,\cdots,p\\[2ex] \dfrac{SIG_{sv}}{\max_{sv} SIG_{sv}}, & s\neq v, s,v=1,\cdots,p\ .\end{cases} \tag{6}$$

If we denote the preselected thresholds for the inputs and interactions by θ_1 and θ_2, respectively, then the significant first-order index set D_1 and the significant second-order index set D_2 can be identified using the relations

$$D_1=\{s|SIG_{ss}>\theta_1, 1\le s\le p\}$$

and

$$D_2=\{(s,v)|SIG_{sv}>\theta_2, 1\le s<v\le p\}\ .$$

TABLE I

Algorithm 1: Cut-HDMR Based on Screening

1. Set ℓ: the level of the sampling matrices
Set r: the number of times the screening is performed
2. For $i=1:r$
A. Call *Algorithm M1* and *Algorithm M2*
B. Evaluate the elementary effect d^i_{sv} using Eqs. (3) and (4)
End For
3. Calculate SIG^* using Eq. (6)
4. Set θ_1 and θ_2, and identify D_1 and D_2
5. Set N_L: number of Lagrange interpolation points
Define Lagrange interpolation points $\{q^k_i\}^{N_L}_{k=1}$ for $i\in D_1, D_2$
6. Pick $\bar{q}$: the reference point
7. Evaluate the response function at
$q=\bar{q}$, $q=\bar{q}\backslash q^k_i$ for $i\in D_1$, $k=1,\cdots,N_L$ and
$q=\bar{q}\backslash\{q^k_i,q^s_j\}$ for $(i,j)\in D_2$, $k,s=1,\cdots,N_L$
8. Form the Cut-HDMR expansion:
$$f(q)\approx f^{cut}(q)=f_0+\sum_{i\in D_1}f_i(q_i)+\sum_{(i,j)\in D_2}f_{ij}(q_i,q_j)\ . \tag{7}$$

V. CUT-HDMR BASED ON SCREENING

We summarize the Cut-HDMR expansion based on the screening in Table I.

We note that the required number of model runs to construct the expansion (7) in *Algorithm 1* is

$$r\left((p+1)+\frac{p(p+1)}{2}+1\right)+|D_1|(N_L-1)+|D_2|(N_L-1)^2,$$

where D_1 and D_2 are the cardinality of D_1 and D_2, respectively. The first $(p+1)$ and the second $\frac{p(p+1)}{2}+1$ are used to find the first- and second-order elementary effects, respectively. The last two expressions in the sum are due to the Lagrange interpolations.

VI. NUMERICAL TEST

To test the performance of *Algorithm 1*, we apply it to a 1-D transport equation detailed in Sec. II. We consider both the accuracy and efficiency of the algorithm.

Let us consider the 1-D transport equation for a two-media U-D_2 reactor moderated by H_2O. The setup of the computational domain is shown in Fig. 2. The parameter values that yield a critical reactor are given in Table II. These values are also the means of the cross sections. This setup (geometry domain together with the parameter values) can be used as a benchmark test for code verification of the transport equation.[17] Note that we make no assumptions regarding the parameter distribution. To construct a Cut-HDMR, we employ (a) the mean of the inputs that is used as the reference point in the expansion and (b) the domain of the input space that is shown in Table II.

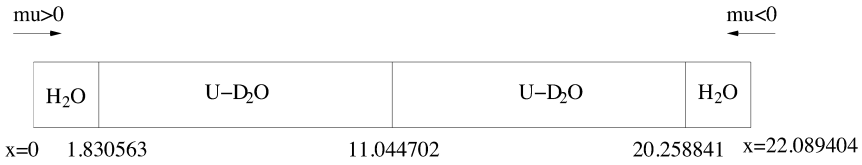

Fig. 2. Schematic of the geometry domain of the test problem.

TABLE II

Mean and Domain of the Scatter/Fission/Capture Cross Sections Used in the Numerical Test*

Material	Σ_s	Σ_f	Σ_c	Σ_t
U-D_2O	0.464338 (0.278603, 0.650073)	0.054628 (0.032777, 0.076479)	0.027314 (0.016388, 0.038240)	0.54628 (0.327768, 0.764792)
H_2O	0.491652 (0.294991, 0.688313)	0.0 —	0.054628 (0.032777, 0.076479)	0.54628 (0.327768, 0.764792)

*The parameter c is the secondaries ratio that measures the mean number of secondary neutrons produced per neutron reaction and is defined by $c = \frac{\Sigma_s + \nu\Sigma_f}{\Sigma_t}$. It is set to be 1.02 for U-D_2O and 0 for H_2O. The parameter ν is set to be 1.7 for U-D_2O and 0 for H_2O. Note that parameters c and ν are not considered as model parameters and therefore are fixed as constants.

Taking $\mu = 8$ and $N_x = 200$ and using the mean of the material values reported in Table II yield the effective eigenvalue, $k_{eff} = 0.99943$, and the corresponding scalar flux is shown in Fig. 3. Following Sood et al.,[17] the flux vector is scaled with respect to its value at the center of the slab. The number of mean free paths of this problem is 12.067. The total number of inputs of this problem is 600.

The first step is to perform screening. As demonstrated by Cropp and Braddock,[9] using small numbers of runs (small r) at quite coarse resolutions (small ℓ) provides very good estimates to the significance of the parameters. We thus take $r = 4$, $\ell = 6$, and $\Delta = 1$. The first-order indices (the diagonal elements of SIG^*) are plotted in Figs. 4a, 4b, and 4c. We observe that the most influential parameters are the capture and fission cross sections near the center of the core. Setting $\theta_1 = 0.4$ yields 213 (out of 600) significant parameters. The second-order indices of the capture cross sections are plotted in Fig. 4d. Note that all other interactions are very weak and therefore are not shown in the plot. We observe that the capture cross sections near the center of the core interact with themselves. Setting $\theta_2 = 0.4$ yields 239 (out of 179 700) significant interactions.

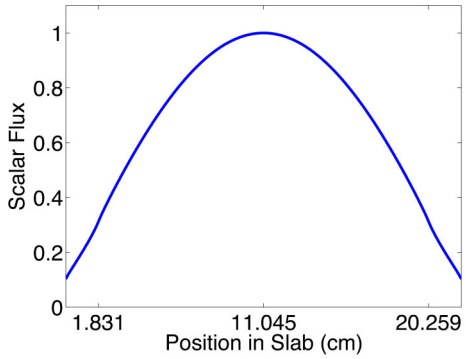

Fig. 3. The scalar flux of the test problem.

Once the significant parameters and interactions are identified, we construct the Cut-HDMR expansion, $f^{cut}(q)$, using Eq. (7) in *Algorithm 1* with N_L set to 5. We then compare $f^{cut}(q)$ with the full model $f(q)$ at 100 000 randomly generated points in the input domain. Table III shows the mean, standard deviation, and skewness calculated by MC, zeroth-order Cut-HDMR, first-order Cut-HDMR, and second-order Cut-HDMR. Note that the standard deviation and skewness cannot be estimated using the zeroth-order expansion. We observe from Table III that the mean of the response (0.9999) is close to the response of the mean of the parameters (0.9994). This indicates that the relation between the inputs and response of this problem is almost linear. Second, adding the significant first-order terms to the Cut-HDMR expansion improves the approximation to the mean as well as yields a very good approximation to the standard deviation. Finally, adding the pairwise interactions into the Cut-HDMR does not improve the estimate to either mean or standard deviation. It does, however, improve the approximation to the skewness.

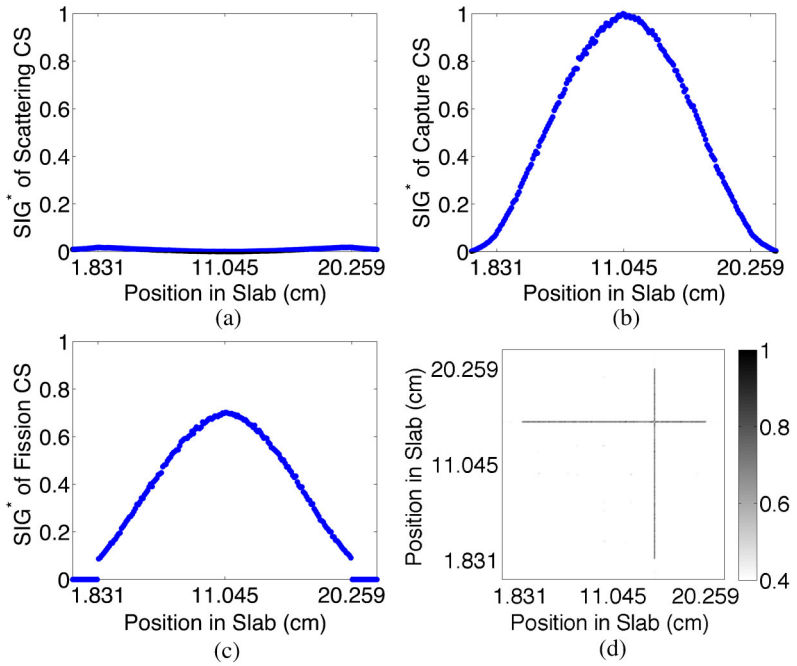

Fig. 4. Statistical significance index *SIG**. (a) The first-order index for scattering cross sections, (b) the first-order index for capture cross sections, (c) the first-order index for fission cross sections, and (d) the second-order index for capture cross sections. All other interactions are small and therefore are not shown.

The time spent to calculate the responses at these 100 000 sampling points is also reported in Table III. We observe that the first-order Cut-HDMR expansion is extremely efficient. We note that the time reported for the Cut-HDMR expansion does not include the time spent for screening, which took $\sim$4 days for this case. One reason for such a lengthy calculation is that *Algorithm 1* was implemented sequentially (four trajectories were constructed sequentially). One can easily expedite the screening process by constructing the four trajectories simultaneously using parallel computing.

To further demonstrate the accuracy of Cut-HDMR expansion, we report the maximum relative error between the Monte Carlo simulations and the expansions in Table IV. The maximum relative error is defined as $\frac{\max|f(q)-f^{cut}(q)|}{\max|f(q)|}$. We observe that the first-order expansion approximates the response accurately and adding the second-order terms into the expansion does decrease the maximum relative error.

VII. CONCLUDING REMARKS

We introduced an algorithm that utilizes first- and second-order Morris screening to first reduce the parameter space to include only the significant parameters and interactions between parameters. A surrogate model

TABLE III

Mean, Standard Deviation, and Skewness of the Effective Eigenvalues Calculated by MC and Cut-HDMR*

	MC	Zeroth-Order Cut	First-Order Cut	Second-Order Cut
Mean	0.9999	0.9994	0.9999	0.9999
Standard deviation	0.0101	—	0.0095	0.0095
Skewness	−0.0431	—	−0.2634	−0.0134
Time (s)	67397	0.6	902	4168

*Three Cut-HDMR expansions (zeroth, first, and second order) are reported. The time reported for the Cut-HDMR does not include the time spent to perform screening but rather the time spent to evaluate 100 000 points using the Cut-HDMR expansion.

TABLE IV

Maximum Relative Error of the Effective Eigenvalues for the 100 000 Sampling Points Calculated by Cut-HDMR*

	Zeroth-Order Cut	First-Order Cut	Second-Order Cut
Maximum relative error (%)	4.9168	1.4624	1.4514

*Three Cut-HDMR expansions (zeroth, first, and second order) are reported.

based on the Cut-HDMR expansions can then be constructed within the reduced space. The algorithm was tested on the 1-D neutron transport equation. The numerical tests have shown that the screening algorithm can successfully identify significant parameters and interactions between parameters. The Cut-HDMR surrogate model constructed based on the significant parameters and interactions accurately and efficiently approximates the full model.

There are several issues to be addressed in future research. The 1-D model considered here neglects the contributions of multiple energy groups and anisotropic geometric and source contributions. Furthermore, we have normalized with regard to the computed flux at the center of the slab rather than with respect to an externally applied power distribution. Hence, while the 1-D model provides a means of illustrating issues of the type encountered in a reactor, it does not accurately model the critical reactor quantities of interest. To achieve this, one must employ 3-D models and codes such as the Oak Ridge National Laboratory package DENOVO. The implementation of these algorithms for DENOVO constitutes one component of future research. An aspect of this research should focus on quantifying the accuracy of the CUT-HDMR expansions for the 3-D models.

As detailed in Sec. I, Cut-HDMR resembles the perturbation methods of Cacuci[10] and Proctor[11] in the sense that both rely on point evaluations at anchor or nominal parameter values to construct second-order surrogate models. A novelty of the proposed algorithm lies in the use of improved Morris screening to determine a subset of influential parameters. Once this parameter set has been determined, a second future research avenue will focus on comparing the accuracy and efficiency of second-order surrogate models obtained using Cut-HDMR and perturbation methods based on truncated Taylor expansions.

ACKNOWLEDGMENTS

This research was supported in part by the U.S. Department of Energy Consortium for Advanced Simulation of Light Water Reactors through grant DE-AC05-00OR22725. It was also supported by the Air Force Office of Scientific Research through grant AFOSR FA9550-11-1-0152.

REFERENCES

1. H. RABITZ and O. F. ALIS, "General Foundation of High Dimensional Model Representations," *J. Math. Chem.*, **25**, 197 (1999); http://dx.doi.org/10.1023/A:1019188517934.

2. J. SHORTER, C. I. PRECILA, and H. RABITZ, "An Efficient Chemical Kinetics Solver Using High Dimensional Model Representations," *J. Phys. Chem. A*, **103**, *36*, 7192 (1999); http://dx.doi.org/10.1021/jp9843398.

3. S. W. WANG et al., "Fully Equivalent Operational Models for Atmospheric Chemical Kinetics Within Global Chemistry-Transport Models," *J. Geophys. Res.*, **104**, *D23*, 30417 (1999); http://dx.doi.org/10.1029/1999JD900830.

4. G. LI, C. ROSENTHAL, and H. RABITZ, "High Dimensional Model Representations," *J. Phys. Chem. A*, **105**, *33*, 7765 (2001); http://dx.doi.org/10.1021/jp010450t.

5. H. RABITZ et al., "Efficient Input-Output Model Representations," *Comput. Phys. Comm.*, **117**, 11 (1999); http://dx.doi.org/10.1016/S0010-4655(98)00152-0.

6. Y. CAO, Z. CHEN, and M. GUNZBURGER, "ANOVA Expansions and Efficient Sampling Methods for Parameter Dependent Nonlinear PDEs," *Int. J. Numer. Anal. Model*, **6**, 256 (2009).

7. I. M. SOBOL, "Theorems and Examples on High Dimensional Model Representation," *Reliab. Eng. Syst. Safety*, **79**, 187 (2003); http://dx.doi.org/10.1016/S0951-8320(02)00229-6.

8. F. CAMPOLONGO and R. D. BRADDOCK, "The Use of Graph Theory in the Sensitivity Analysis of the Model Output: A Second Order Screening Method," *Reliab. Eng. Syst. Safety*, **64**, 1 (1999); http://dx.doi.org/10.1016/S0951-8320(98)00008-8.

9. R. A. CROPP and R. D. BRADDOCK, "The New Morris Method: An Efficient Second-Order Screening Method," *Reliab. Eng. Syst. Safety*, **78**, 77 (2002); http://dx.doi.org/10.1016/S0951-8320(02)00109-6.

10. D. G. CACUCI, *Sensitivity and Uncertainty Analysis: Theory*, Chapman and Hall/CRC, Boca Raton, Florida (2003).

11. W. C. PROCTOR, "Elements of High-Order Predictive Model Calibration Algorithms with Applications to Large-Scale Reactor Physics Systems," PhD Dissertation, North Carolina State University (Mar. 27, 2012).

12. M. L. ADAMS and E. W. LARSEN, "Fast Iterative Methods for Discrete-Ordinates Particle Transport Calculations," *Prog. Nucl. Energy*, **40**, *1*, 3 (2002); http://dx.doi.org/10.1016/S0149-1970(01)00023-3.

13. T. M. SUTTON, "Wielandt Iteration as Applied to the Nodal Expansion Method," *Nucl. Sci. Eng.*, **98**, 169 (1988); http://dx.doi.org/10.13182/NSE88-1.

14. O. F. ALIS and H. RABITZ, "Efficient Implementation of High Dimensional Model Representations," *J. Math. Chem.*, **29**, *2*, 127 (2001); http://dx.doi.org/10.1023/A:1010979129659.

15. M. MORRIS, "Factorial Sampling Plans for Preliminary Computational Experiments," *Technometrics*, **33**, *2*, 161 (1991); http://dx.doi.org/10.1080/00401706.1991.10484804.

16. F. CAMPOLONGO and A. SALTELLI, "Sensitivity Analysis of an Environmental Model: An Application of Different Analysis Methods," *Reliab. Eng. Syst. Safety*, **57**, *1*, 49 (1997); http://dx.doi.org/10.1016/S0951-8320(97)00021-5.

17. A. SOOD, R. A. FORSTER, and D. K. PARSONS, "Analytical Benchmark Test Set For Criticality Code Verification," *Prog. Nucl. Energy*, **42**, *1*, 55 (2003); http://dx.doi.org/10.1016/S0149-1970(02)00098-7.